Extraocular muscle positions in anterior plagiocephaly: V-pattern strabismus explained using geometric mophometrics

Romain Touzé, Yann Heuzé, Matthieu Robert, Dominique Brémond-Gignac, Charles-Joris Roux, Syril James, Giovanna Paternoster, Eric Arnaud, Roman Hossein Khonsari

British Journal of Ophthalmology

Extra-ocular muscle positions in anterior plagiocephaly; V-pattern strabismus explained using geometric mophometrics

Journal:	*British Journal of Ophthalmology*
Manuscript ID	bjophthalmol-2019-314989.R1
Article Type:	Clinical science
Date Submitted by the Author:	n/a
Complete List of Authors:	Touzé, Romain; Hopital Necker-Enfants Malades, Ophthalmology Heuzé, Yann; CRNS, Université de Bordeaux Robert, Matthieu; Hopital universitaire Necker-Enfants malades Maladies rares et chroniques, Ophthalmology Bremond Gignac, Dominique; University Hospital, Necker enfants maladies, Ophthalmology; Paris V René Descartes University, CNRS Unit FR3636 Roux, Charles-Joris; Hopital Necker-Enfants Malades, Pediatric Radiology James, Syril; Hopital Necker-Enfants Malades, Neurosurgery; Clinique Marcel Sembat, Neurosurgery Paternoster, Giovanna; Hopital Necker-Enfants Malades, Neurosurgery Arnaud, Eric; Hopital Necker-Enfants Malades, Neurosurgery; Clinique Marcel Sembat, Neurosurgery Khonsari, Roman Hossein; Hopital Necker-Enfants Malades, Maxillo-facial and plastic surgery unit
Keywords:	Child health (paediatrics), Imaging, Muscles, Orbit, Treatment Surgery

Title page

Extra-ocular muscle positions in anterior plagiocephaly; V-pattern strabismus explained using geometric mophometrics

Short title V-pattern strabismus in anterior plagiocephaly

Romain **Touzé**[1*], Yann **Heuzé**[2], Matthieu P. **Robert**[1,3], Dominique **Brémond-Gignac**[1], Charles-Joris **Roux**[4], Syril **James**[5,6], Giovanna **Paternoster**[5], Eric **Arnaud**[5,6], Roman Hossein **Khonsari**[7]

1. Service d'ophtalmologie, Hôpital Universitaire Necker – Enfants Malades, Assistance Publique – Hôpitaux de Paris ; Université de Paris, Sorbonne Paris Cité ; Paris, France
2. CNRS, Université de Bordeaux, MCC, PACEA, UMR5199, Pessac, France
3. COGNAC-G, UMR 8257 CNRS-SSA-Université de Paris, Paris, France
4. Service de radiologie, Hôpital Universitaire Necker – Enfants Malades, Assistance Publique – Hôpitaux de Paris ; Université de Paris, Sorbonne Paris Cité ; Paris, France
5. Service de neurochirurgie, Unité Fonctionnelle de Chirurgie Craniofaciale, Hôpital Universitaire Necker – Enfants Malades, Assistance Publique – Hôpitaux de Paris ; Centre de Référence des Malformations Craniofaciale CRANIOST, Filière Maladies Rares TeteCou ; Université de Paris, Sorbonne Paris Cité ; Paris, France
6. Clinique Marcel Sembat, Ramsay – Générale de Santé, Boulogne-Billancourt, France
7. Service de chirurgie maxillo-faciale et chirurgie plastique, Hôpital Universitaire Necker – Enfants Malades, Assistance Publique – Hôpitaux de Paris ; Centre de Référence des Malformations Rares de la Face et de la Cavité Buccale MAFACE, Filière Maladies Rares TeteCou ; Université de Paris, Sorbonne Paris Cité ; Paris, France

Keywords: Child health (paediatrics); Imaging; Muscles; Orbit; Treatment Surgery

Number of Tables: 1
Number of Figures: 4
Word count of Abstract: 243
Word count of Paper: 2440

Corresponding Author:

Dr Romain Touzé
Service d'ophtalmologie, Hôpital Universitaire Necker - Enfants Malades, 149, Rue de Sèvres, 75015 Paris. France
Email r.touze.rt@gmail.com Tel + 33629654980

Synopsis:

This study reports statistically abnormal extra-oculomotor muscles positions within the orbit of patients with anterior plagiocephaly using the geometric morphometrics, in order to better understand strabismus in this pathology especially V-pattern.

Abstract

Introduction

Ophthalmological involvement in anterior plagiocephaly (AP) due to unicoronal synostosis (UCS) raises management challenges. Two abnormalities of the extra-ocular muscles (EOM) are commonly reported in UCS without objective quantification: (1) malposition of the trochlea of the superior oblique muscle and (2) excyclorotation of the eye. Here we aimed to assess the positions of the EOM in AP, using geometric morphometrics based on magnetic resonance imaging (MRI) data.

Materials and Methods

Patient files were listed using Dr WareHouse, a dedicated big data search engine. We included all patients with AP managed between 2013 and 2018, with an available digital pre-operative MRI. MRIs from age-matched controls without craniofacial conditions were also included. We defined 13 orbital and skull base landmarks in order to model the 3D position of the EOM. Cephalometric analyses and geometric morphometrics with Procrustes superimposition and principal component analysis were used with the aim of defining specific EOM anomalies in UCS.

Results

We included 15 pre-operative and 7 post-operative MRIs from patients with UCS and 24 MRIs from age-matched controls. Cephalometric analyses, Procrustes superimposition and distance computations showed a significant shape difference for the position of the trochlea of the superior oblique muscle and an excyclorotation of the EOM.

Conclusion

Our results confirm that UCS-associated anomalies of the superior oblique muscle function are associated with a malposition of its trochlea in the roof of the orbit. This clinical anomaly supports the importance of MRI imaging in the surgical management of strabismus in patients with UCS.

Introduction

Craniosynostoses are often associated with strabismus. The management of these specific types of strabismus is a clinical challenge, especially in anterior plagiocephaly (AP) caused by unicoronal synostosis (UCS). UCS is the third most common single-suture craniosynostosis and is associated with the premature unilateral fusion of a coronal suture. Craniofacial anomalies in UCS include a larger orbit on the affected side, a shift of the petrous bone towards the fused suture, compensatory growth of the contralateral forehead and temporal bone, and contralateral deviation of the vomer and nasal pyramid.[1]

Ocular involvement is frequent in UCS and includes extra-ocular muscle (EOM) dysfunction with cyclovertical strabismus, astigmatism - usually contralateral to the UCS, due to the compensatory deformations of the contralateral bones - with anisometropia, and amblyopia. The prevalence of ocular abnormalities ranges from 50 to 65% in this condition.[2–4] This high prevalence underlines the need for a systematic ophthalmological clinical screening for patients with UCS within multidisciplinary craniofacial teams, in order to prevent, detect, and treat the amblyopia.

The most common type of strabismus in UCS is referred to as the V-pattern, which is defined by a vertical incomitance with a distance between both eyes larger in upgaze than in downgaze.[2,5] Two hypotheses have been proposed in the literature in order to explain the occurrence of V-pattern oculomotor anomalies in UCS: (1) excyclorotation of the rectus muscle and (2) inferior oblique overaction associated with superior oblique underaction.[1,2,6,7]

Here we assessed the positions of the EOM in patients with UCS and controls, based on MRI data and geometric morphometric analyses, and screened for clinically relevant specificities of the muscular anatomy of UCS orbits.

Geometric morphometrics allowed us to acquire, process and analyze landmarks by preserving their 3D inter-relationship. This approach was required as we had to compare non-trivial shapes.[8] The framework used to assess our data was Procrustes superimposition followed by Principal Component Analysis (PCA). Procrustes superimposition allowed comparing different shapes by freely adjusting the position, orientation and scale parameters using translations, reflections and rotations.[9] PCA was used to reduce the large number of variables responsible for shape differences into a small number of principal variables with geometric correspondence.[10]

Our aim was to find anatomical bases for the V-pattern strabismus. More precisely, we assessed the 3D modifications in the positions of EOM in UCS and the effects of fronto-orbital advancement surgery on these positions.

Material and Methods

Clinical data

We retrospectively included patients with isolated UCS and with at least one available digital pre-operative craniofacial magnetic resonance imaging (MRI), managed in our tertiary center (French National Reference Center for Craniofacial Malformations - CRANIOST) between 2013 and 2018, using Dr Warehouse search engine.[11] We excluded patients with complex and syndromic craniosynostosis and deformational plagiocephaly. Age-matched control patients without craniofacial anomalies were also retrospectively included. We analyzed the effects of fronto-orbital advancement surgery based on post-operative MRIs for included patients, when available. For image analysis purposes, we mirrored patients with left UCS in order to consider a cohort of patients with right UCS only.[12] All patients with UCS benefited from fronto-orbital advancement.

Morphometrics

Landmarking was performed using Avizo 6.4.0 (Thermo Fisher Scientific, Waltham, Massachusetts, USA). Landmarks were placed using Multi Planar Reconstruction (MPR) on Cube T1-weighted or Cube T2-weighted sequences. Twelve bilateral orbital landmarks were defined: (1; 5) right and left lateral rectus; (2; 6) right and left superior rectus; (3; 7) right and left medial rectus; (4; 8) right and left inferior rectus; (9; 10) right and left optic nerve; (11; 12) right and left superior oblique trochlea. One extra-orbital landmark was also defined: (13) chiasma (Table 1). Landmarks 1-10 were placed using coronal views, on the plane immediately

behind the two globes (Figure 1). Pulleys of recti muscles were described in dynamic MRI (IMROD) as encircling sleeves and rings of collagen in the tenon fascia.[13]

Table 1.

Number	Anatomical definition
1	Right lateral rectus chiasma
2	Right superior rectus
3	Right medial rectus
4	Right inferior rectus
5	Left lateral rectus chiasma
6	Left superior rectus
7	Left medial rectus
8	Left inferior rectus
9	Right optic nerve
10	Left optic nerve
11	Right superior oblique trochlea
12	Left superior oblique trochlea
13	Chiasma

Table 1. Orbital and extra-orbital landmarks used to model the 3D position of extra-ocular muscles in anterior plagiocephaly.

These pulleys represented the functional vector of EOMs and were located more proximal relative to muscle insertions. That's why we determined the coronal plane sectioning these pulleys to place landmarks concerning recti muscles. Landmarks 11 and 12 were defined using MPR after having localized the trochlea of the superior oblique muscle. Landmark 13 (chiasma) was placed using coronal sections.

We exported all landmark coordinates from Avizo to MorphoJ [14] in order to perform geometric morphometric analyses.[8] We extracted the shape information defined by the

landmarks and performed a generalized Procrustes superimposition.[9] Procrustes shape coordinates were analyzed using a principal components analysis (PCA).[10] Shape differences between groups were assessed based on Procrustes distances (d) with a permutation test of 10,000 rounds to test the statistical significance of d.[8]

We furthermore performed cephalometrics analyses in 2D defining angles and linear distances between landmarks in using coronal and axial planes. These angles and distances were determined using Euclidian distances and scalar products, and compared between UCS and controls. We defined two vectors named *u* (landmark 2 to 4) and *v* (landmark 1 to 3) in the coronal plane. Angle α between *u* and *v* was computed using the scalar product. We furthermore computed the angles β between *u* and the x-axis, and the angle γ between *v* and the x-axis (Resumed in the Figure 3).

Data analysis

Data analysis was performed using R3.3.3.[15] Comparisons of means were performed using a Wilcoxon test, depending on the data distribution and **s**ignificance was defined for $p<0.05$. We performed a reproducibility assessment based on a subset of 10 normal MRIs. Two operators (for the interobserver reproducibility) (RT and RHK) landmarked these MRIs three consecutive times (intraobserver reproducibility). The *concordance correlation coefficient* (CCC) agreement of Lin [16] was computed for each operator and landmark. An *overall concordance correlation coefficient* (OCCC) was also computed.[17] CCC and OCCC values above 0.99 corresponded to excellent reproducibility of landmark placement.[16]

Results

We selected 26 patients with UCS; we excluded 10 patients because of low quality MRI images and 1 patient with a late diagnosis of complex craniosynostosis to finally include 15 patients with MRI data before any cranio-facial surgery. The mean age of the 15 remaining patients (30 orbits) was 11.9 ± 5.7 months (4-22 months). We included 24 (48 orbits) age-matched controls, with a mean age of 13.4 ± 5.8 months (6-23 months) (p=0.61). Among the 15 included patients with UCS, 7 had a digital post-operative MRI (14 orbits) performed 1 month after the surgical procedure (fronto-orbital advancement). The mean age of patients with post-operative MRIs was 17 ± 5.3 months (13-25 months). None of these 7 patients had EOM surgery performed before post-operative MRIs.

The CCC for each landmark and OCCC were above 0.99, indicating reliable landmark placement for all landmarks and the two operators.

The PCA found shape's difference between both groups. The first five principal components (PCs) accounted for more than 70% of the total variance (Supplementary Figure 1). Both groups were well separated with the two first PCs (Supplementary Figure 2). The Procrustes distance between UCS and control was significant ($d=0.11$, $p < 0.01$). We observed an abnormal location of the superior oblique trochlea in the UCS orbit, corresponding to a lateral, superior and posterior displacement within the orbit (Figure 2-3). We furthermore observed a significant excyclorotation in the UCS group, affecting the recti muscles, more pronounced on the side where the suture was closed. In UCS, the superior rectus was displaced laterally, the inferior rectus was displaced medially, the lateral rectus downward, and the medial rectus upward in the coronal plane (Figure 3).

Euclidian distances between landmark 11 (right superior oblique trochlea) and landmark 9 (right optic nerve) were smaller in the UCS group compared to control group: respectively 18.9 mm ± 1.7 mm *vs.* 20.6 mm ± 1.4 mm (p = 0.002; IC95% [0.77; ∞]), which confirmed the lateral (coronal plane) and posterior (axial plane) displacement of the trochlea within the orbit.

Mean α was significantly different between control and UCS groups: 81.3° ± 4.6° vs 74.3° ±8.6° respectively (p=0.008; IC95% [2.1; 12.2]). Mean β was significantly different between control and UCS groups: 82.4° ± 5.2° vs 66.3° ±8.1° respectively (p<0.001; IC95% [11.1; 20.9]). Mean γ was significantly different between control and UCS groups: 0.9° ± 3.7° vs 7.9° ± 7.2° respectively (p<0.001: IC95% [-13.0; -4.7]). α and β were smaller in the UCS group relative to controls; γ values were larger in the UCS group relative to controls.

Among the 15 patients included, 7 patients had an MRI performed before and after Fronto-facial advancement. In this subgroup of patients, we observed a qualitative decrease of the excyclorotation of the recti muscles after surgery: the superior oblique muscle was displaced downward and medially compared to the pattern before surgery, which corresponded to a trend towards normalization (Figure 4). Nevertheless, we could not confirm this shape modification quantitatively because we found a Procrustes distance at 0.05 with a p-value (10000 permutations) of 0.07.

Discussion

The management of strabismus in craniosynostosis, and particularly in UCS, is a challenge as its mechanisms are not clearly established and because of the massive orbital remodeling caused by craniofacial surgical procedures, such as fronto-orbital advancement.

The high prevalence of strabismus in UCS is well-established: in their cohort of 59 UCS patients, MacIntosh *et al.* [2] found 57.6% of strabismus, 61% of which were esotropia with a vertical component, with 50.8% of inferior oblique overaction / superior oblique underaction.

In a recent review Ron et Dagi [18] summarized all hypotheses explaining V-pattern strabismus in craniosynostoses and pinpointed two main theories as the most satisfactory : (1) inferior oblique overaction / superior oblique underaction induced by the orbital deformation, and (2) excyclorotation of the recti EOM, also induced by the orbital deformation. Nischal *et al.* [19] proposed a three-step theory in order to explain the origins of this specific type of strabismus in UCS: (1) frontal retrusion on the side with coronal synostosis, (2) secondary displacement of the trochlea of the superior oblique muscle, (3) causing a mechanical disadvantage for the superior oblique muscle and an overaction of the inferior oblique. However, Cheng *et al.*[20] argued that the V-pattern vertical component or the upshoot in adduction could not be explained by the inferior oblique overaction / superior oblique underaction only. For these authors, the excyclorotation induced by the deformation of the orbit was also involved in the origin of the strabismus. They demonstrated the excyclorotation of the EOM in several cases of craniosynostosis - the medial rectus being displaced upward, the lateral rectus downward, the inferior rectus medially and the superior rectus laterally. Tan *et al.* [21] studied the upshoot in adduction in order to determine its causes, based on a cohort of 40 patients with various forms of craniosynostosis, including 9 patients with UCS. Among these 9 patients with UCS, 6 patients had an upshoot in adduction. They found that the angle of excyclorotation was more

pronounced in patients with upshoot in adduction, based on comparisons with the non-affected side.

Here, we provide for the first-time quantitative data on the average position of the EOM in the UCS orbit. We found a significant upward, lateral and backward displacement of the trochlea of the oblique superior muscle. According to the vectorial action of the oblique superior muscle, these displacements were most probably associated with a weaker action of the oblique superior muscle, because the pulley effect of the trochlea was less efficient and a more posterior trochlea induced an upward drift of the globe. We also demonstrated an excyclorotation, in particular affecting the superior rectus (laterally displaced) and the inferior rectus (medially displaced). To our knowledge, this is the first evidence of EOM displacements in UCS based on 3D MRI data, and the first quantitative and objective support of the current theories on the origins of strabismus in UCS.

The displacement of the superior oblique trochlea can induce a pseudo-superior oblique palsy. As any superior oblique palsy - or pseudo superior oblique palsy - causes a true excyclorotation of the globe, [22] hence of the EOM, it is difficult to assess whether the excyclorotation of the EOM found in these patients is an effect of the pseudo-superior oblique palsy resulting from a trochlea displacement, or a direct effect of a bony orbit rotation. In order to answer this question, further study could aim at correlating the bony orbit rotation and the EOM excyclorotation in UCS.

Orbital imaging using MRI in craniosynostosis is a valuable tool for the assessment of strabismus.[23–25] The absence of rectus and/or oblique muscles has been reported in craniosynostosis cases and should be diagnosed before the surgery.[26] Further studies are also needed to better describe the EOM phenotype in other forms of non-syndromic and syndromic craniosynostosis.

According to the literature, surgery on oculomotor muscles should be performed after craniofacial procedures, such as fronto-orbital advancement.[1,19,25,27,28] In a recent review, Alfort *et al.* [29] underlined the specific risk of strabismus secondary to fronto-orbital advancement. Patients are under 12 months of age when undergoing this procedure and oculomotor muscle surgery is usually performed later in age. Our data showed a trend towards normalization for excyclorotation and trochlea position after fronto-orbital advancement in a subgroup of 7 patients. Nevertheless, we were not able to demonstrate this morphological modification and correlate it with clinical effects on strabismus, due to an insufficient number of patients and to the impossibility to precisely quantify cyclovertical strabismus characteristics below one year of age.

To date, no guidelines exist for the management of strabismus in craniosynostoses. The usual procedure to treat inferior oblique overaction consists in weakening the inferior oblique muscle. Some authors, such as Tan et al. [21], have suggested that in cases with significant excyclorotation, a transposition of the inferiorly displaced lateral rectus muscle could be more appropriate to correct the V-pattern.

Limitations

One of the main potential limitations of this study relates to the accuracy of landmark placement. In order evaluate this issue, we assessed intra- and inter-individual reproducibility of landmark placement, as described in the Material and Methods section, and showed the reliability of our landmark placement protocol.

In brief, we quantitatively demonstrated two main EOM modifications associated with UCS: (1) lateral, superior and posterior displacement of the superior oblique trochlea and (2) excyclorotation of the rectus muscles. These anatomical anomalies are reasonable candidates to explain the origins and specificities of strabismus in UCS.

Conclusion

We report the first detailed assessment of EOM positions in anterior plagiocephaly due to unicoronal synostosis. Strabismus in unicoronal synostosis has repeatedly been explained by weakness of the superior oblique muscle due to a malposition of its trochlea and excyclorotation of rectus muscles. Our study provides a quantitative proof of these two anomalies and supports the usual hypothesis formulated in the literature. It underlines the relevance of orbital imaging in the management of strabismus in patients with UCS.

Funding Statement

This research received no specific grant from any funding agency in the public, commercial or not-for-profit sectors.

Competing Interests

None authors have a competing interest

Contributorship Statement

All authors made substantial contributions to conception and design, analysis and interpretation of data; drafted or critically revised the article; and gave final approval of the version to be published.

Data Sharing

N/A

Acknowledgments

Special thanks to strabologists Drs Mitra Goberville and Marie-Andrée Espinasse-Berrod.

Ethical statement

Patients were informed of the use of their medical data for this study.

References

1 Di Rocco C, Paternoster G, Caldarelli M, *et al.* Anterior plagiocephaly: epidemiology, clinical findings,diagnosis, and classification. A review. *Childs Nerv Syst* 2012;**28**:1413–22. doi:10.1007/s00381-012-1845-2

2 MacIntosh C, Wall S, Leach C. Strabismus in unicoronal synostosis: ipsilateral or contralateral? *J Craniofac Surg* 2007;**18**:465–469.

3 Eveleens JRJ, Mathijssen IM, Lequin MH, *et al.* Vertical Position of the Orbits in Nonsyndromic Plagiocephaly in Childhood and Its Relation to Vertical Strabismus: *J Craniofac Surg* 2011;**22**:135–8. doi:10.1097/SCS.0b013e3181f6f814

4 Gupta PC, Foster J, Crowe S, *et al.* Ophthalmologic findings in patients with nonsyndromic plagiocephaly. *J Craniofac Surg* 2003;**14**:529–532.

5 Samra F, Paliga JT, Tahiri Y, *et al.* The prevalence of strabismus in unilateral coronal synostosis. *Childs Nerv Syst* 2015;**31**:589–96. doi:10.1007/s00381-014-2580-7

6 Dagi LR, MacKinnon S, Zurakowski D, *et al.* Rectus muscle excyclorotation and V-pattern strabismus: a quantitative appraisal of clinical relevance in syndromic craniosynostosis. *Br J Ophthalmol* 2017;**101**:1560–5. doi:10.1136/bjophthalmol-2016-309996

7 Bagolini B, Campos EC, Chiesi C. Plagiocephaly Causing Superior Oblique Deficiency and Ocular Torticollis: A New Clinical Entity. *Arch Ophthalmol* 1982;**100**:1093–6. doi:10.1001/archopht.1982.01030040071012

8 Mitteroecker P, Gunz P. Advances in Geometric Morphometrics. *Evol Biol* 2009;**36**:235–47. doi:10.1007/s11692-009-9055-x

9 Rohlf FJ, Slice D. Extensions of the Procrustes Method for the Optimal Superimposition of Landmarks. *Syst Biol* 1990;**39**:40–59. doi:10.2307/2992207

10 Jolliffe I. Principal Component Analysis. In: Lovric M, ed. *International Encyclopedia of Statistical Science*. Berlin, Heidelberg: : Springer Berlin Heidelberg 2011. 1094–6. doi:10.1007/978-3-642-04898-2_455

11 Garcelon N, Neuraz A, Benoit V, *et al.* Improving a full-text search engine: the importance of negation detection and family history context to identify cases in a biomedical data warehouse. *J Am Med Inform Assoc* 2017;**24**:607–13. doi:10.1093/jamia/ocw144

12 Heuzé Y, Martínez-Abadías N, Stella JM, *et al.* Unilateral and bilateral expression of a quantitative trait: asymmetry and symmetry in coronal craniosynostosis. *J Exp Zoolog B Mol Dev Evol* 2012;**318**:109–122.

13 Kono R, Clark RA, Demer JL. Active pulleys: magnetic resonance imaging of rectus muscle paths in tertiary gazes. *Invest Ophthalmol Vis Sci* 2002;**43**:2179–2188.

14 Klingenberg CP. MorphoJ: an integrated software package for geometric morphometrics. *Mol Ecol Resour* 2011;**11**:353–7. doi:10.1111/j.1755-0998.2010.02924.x

15 Team RC. R: A language and environment for statistical computing. R Foundation for Statistical Computing, Vienna, Austria. 2012. *URL Httpwww R-Proj Org* 2018.

16 Lin LI-K. A Concordance Correlation Coefficient to Evaluate Reproducibility. *Biometrics* 1989;**45**:255–68. doi:10.2307/2532051

17 Barnhart HX, Haber M, Song J. Overall Concordance Correlation Coefficient for Evaluating Agreement Among Multiple Observers. *Biometrics* 2002;**58**:1020–7. doi:10.1111/j.0006-341X.2002.01020.x

18 Ron Y, Dagi LR. The etiology of V pattern strabismus in patients with craniosynostosis. *Int Ophthalmol Clin* 2008;**48**:215–223.

19 Nischal KK. Ocular aspects of craniofacial disorders. *Am Orthopt J* 2002;**52**:58–68.

20 Cheng H, Burdon MA, Shun-Shin GA, *et al.* Dissociated eye movements in craniosynostosis: a hypothesis revived. *Br J Ophthalmol* 1993;**77**:563–8. doi:10.1136/bjo.77.9.563

21 Tan KP, Sargent MA, Poskitt KJ, *et al.* Ocular Overelevation in Adduction in Craniosynostosis: Is It the Result of Excyclorotation of the Extraocular Muscles? *J Am Assoc Pediatr Ophthalmol Strabismus* 2005;**9**:550–7. doi:10.1016/j.jaapos.2005.07.004

22 Noorden GK von, Murray E, Wong SY. Superior Oblique Paralysis: A Review of 270 Cases. *Arch Ophthalmol* 1986;**104**:1771–6. doi:10.1001/archopht.1986.01050240045037

23 Clark RA. Orbital Imaging in Strabismus. *J Binocul Vis Ocul Motil* 2018;**68**:87–98. doi:10.1080/2576117X.2018.1486678

24 Clark RA, Demer JL. Magnetic Resonance Imaging of the Effects of Horizontal Rectus Extraocular Muscle Surgery on Pulley and Globe Positions and Stability. *Investig Opthalmology Vis Sci* 2006;**47**:188. doi:10.1167/iovs.05-0498

25 Morax S. Oculo-motor disorders in craniofacial malformations. *J Maxillofac Surg* 1984;**12**:1–10. doi:10.1016/S0301-0503(84)80201-5

26 Diamond GR, Katowitz JA, Whitaker LA, *et al.* Variations in extraocular muscle number and structure in craniofacial dysostosis. *Am J Ophthalmol* 1980;**90**:416–418.

27 Yang B, Ni J, Li B. 3D morphological change of skull base and fronto-temporal soft-tissue in the patients with unicoronal craniosynostosis after fronto-orbital advancement. *Childs Nerv Syst* 2018;**34**:947–55. doi:10.1007/s00381-018-3721-1

28 Simon A, Bocquet E, Pellerin P, *et al.* Three-dimensional study of 31 cases of synostotic anterior plagiocephaly before and after surgical management the Lille protocol. *J Cranio-Maxillofac Surg* 2018;**46**:958–66. doi:10.1016/j.jcms.2018.03.014

29 Alford J, Derderian CA, Smartt JM. Surgical Treatment of Nonsyndromic Unicoronal Craniosynostosis: *J Craniofac Surg* 2018;:1. doi:10.1097/SCS.0000000000004509

410

411

412

Figure legends

Figure 1. 3D positioning of the landmarks based on MRI images. A. Red line: section plane used to place rectus muscle landmarks. B. Rectus muscle landmarks (red dots) and optic nerve landmarks (dark green dots). C. Trochlea of superior oblique muscles (yellow circles). D,E. Trochlea of superior oblique muscles (yellow dots). F. Chiasma landmark (blue dot); rectus muscle landmarks (red dots); optic nerve landmarks (dark green dots); trochlea of superior oblique muscles (yellow dots).

Figure 2. A. Procrustes superimposition in axial view for controls; right trochlea of the superior oblique muscle: red arrow. B. Procrustes superimposition in coronal view for controls; right trochlea of the superior oblique muscle: red arrow. C. Procrustes superimposition in sagittal view for controls. D. Procrustes superimposition in axial view for anterior plagiocephaly; right trochlea of the superior oblique muscle: red arrow. E. Procrustes superimposition in coronal view for anterior plagiocephaly; right trochlea of the superior oblique muscle: red arrow. F. Procrustes superimposition in sagittal view for anterior plagiocephaly.

Figure 3. A. Landmarks in a control case displayed on a coronal MRI section. B. Landmarks in an anterior placiocephaly case displayed on a coronal MRI section. Exclycloratation quantified using angles α, β and γ; right trochlea of superior oblique muscle: red arrow.

Figure 4. A. Coronal MRI section in anterior plagiocephaly before fronto-orbital advancement. B. Coronal MRI section in anterior plagiocephaly after fronto-orbital advancement. Qualitative correction of the position of the right trochlea of the superior oblique muscle (red arrow) and qualitative reduction of the excyclorotation of rectus muscles.

Figure legends supplementary files

Figure 1. Variance

A diagram showing the percentages of total variance for which the principal components (PCs) account. The five first PCs represent more than 70% of the total difference between both groups.

Figure 2. PCA

Principal component analysis with Procrustes superimposition of the two groups (UCS) and control. We can observe difference with confidence ellipses concerning PC1 vs PC2; PC1 vs PC4; and PC1 vs PC5.

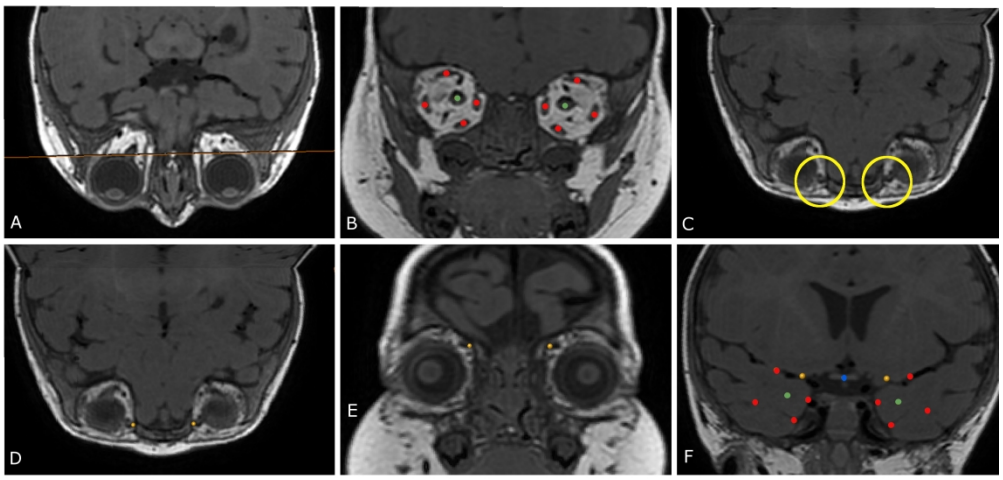

Figure 1. 3D positioning of the landmarks based on MRI images. A. Red line: section plane used to place rectus muscle landmarks. B. Rectus muscle landmarks (red dots) and optic nerve landmarks (dark green dots). C. Trochlea of superior oblique muscles (yellow circles). D,E. Trochlea of superior oblique muscles (yellow dots). F. Chiasma landmark (blue dot); rectus muscle landmarks (red dots); optic nerve landmarks (dark green dots); trochlea of superior oblique muscles (yellow dots).

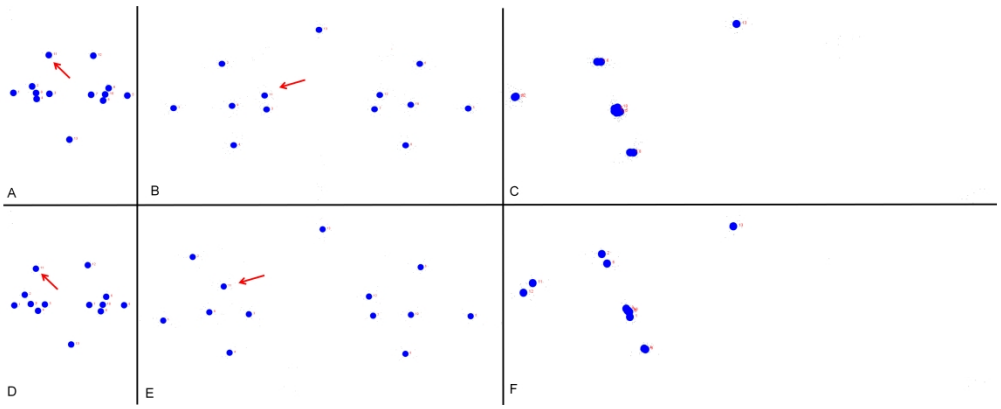

Figure 2. A. Procrustes superimposition in axial view for controls; right trochlea of the superior oblique muscle: red arrow. B. Procrustes superimposition in coronal view for controls; right trochlea of the superior oblique muscle: red arrow. C. Procrustes superimposition in sagittal view for controls. D. Procrustes superimposition in axial view for anterior plagiocephaly; right trochlea of the superior oblique muscle: red arrow. E. Procrustes superimposition in coronal view for anterior plagiocephaly; right trochlea of the superior oblique muscle: red arrow. F. Procrustes superimposition in sagittal view for anterior plagiocephaly.

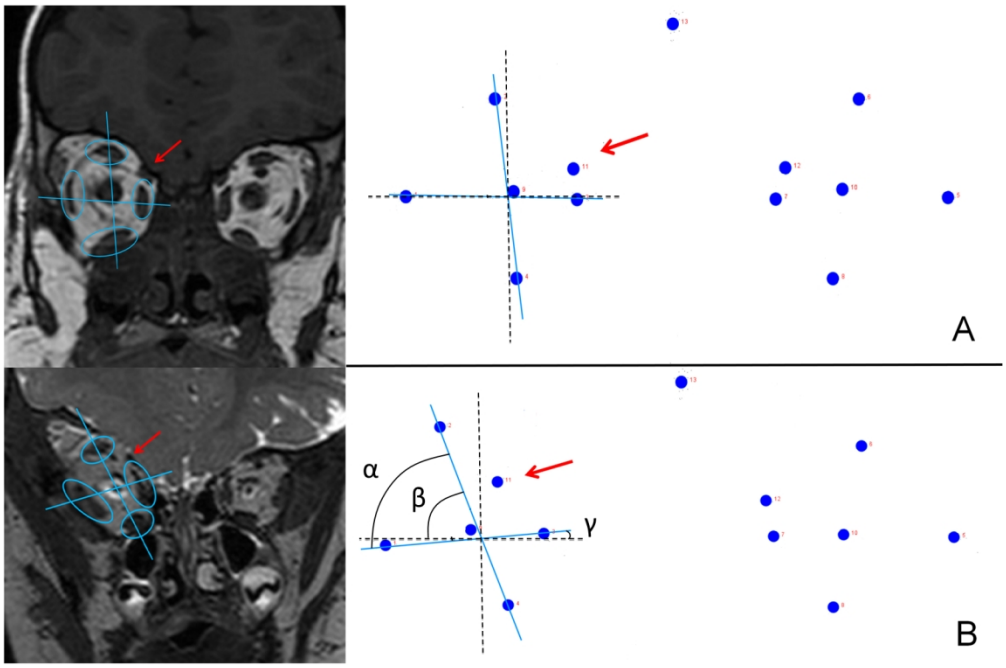

Figure 3. A. Landmarks in a control case displayed on a coronal MRI section. B. Landmarks in an anterior plagiocephaly case displayed on a coronal MRI section. Exclycloratation quantified using angles α, β and γ; right trochlea of superior oblique muscle: red arrow.

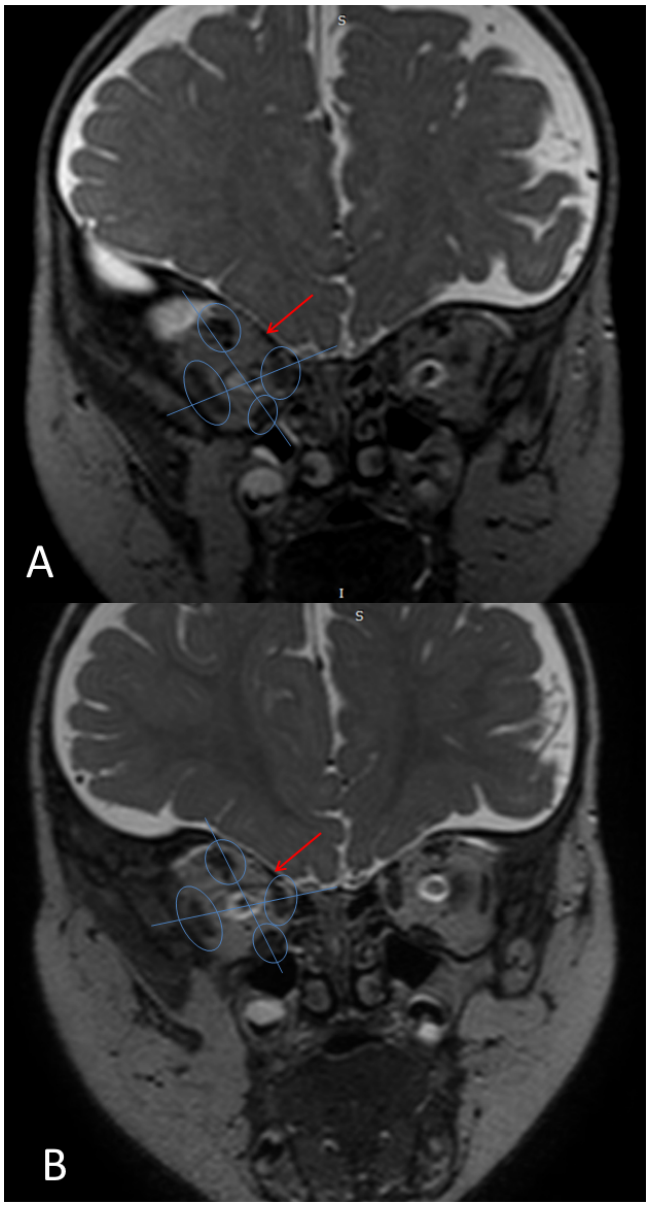

Figure 4. A. Coronal MRI section in anterior plagiocephaly before fronto-orbital advancement. B. Coronal MRI section in anterior plagiocephaly after fronto-orbital advancement. Qualitative correction of the position of the right trochlea of the superior oblique muscle (red arrow) and qualitative reduction of the excyclorotation of recti muscles.

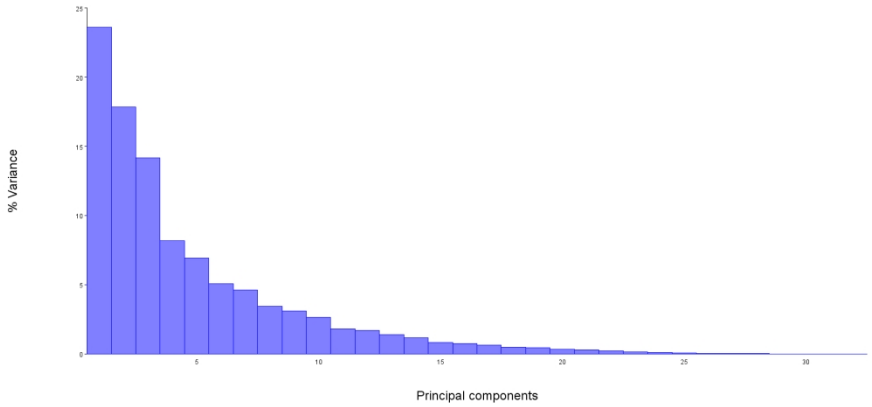

672x310mm (72 x 72 DPI)

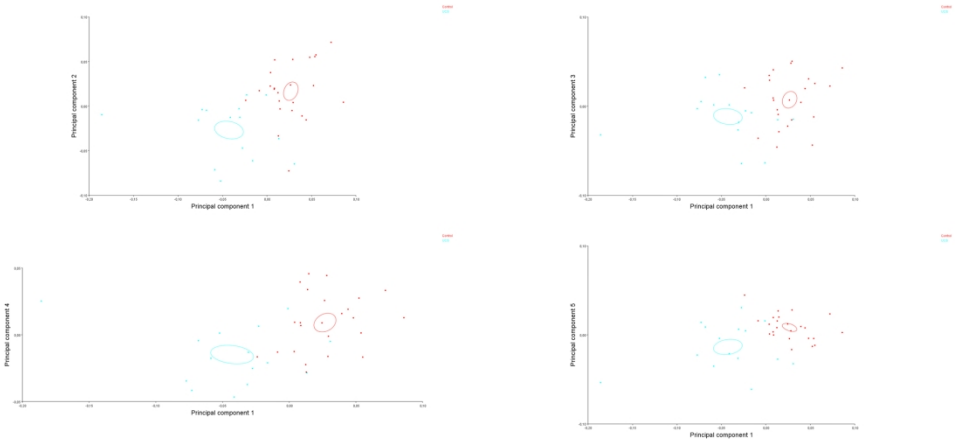
Principal component 2
Principal component 1
Principal component 3
Principal component 1
Principal component 4
Principal component 1
Principal component 5
Principal component 1